Geophysical Journal International

Geophys. J. Int. (2019) **218,** 1442–1455
Advance Access publication 2019 May 17
GJI Geomagnetism, rock magnetism and palaeomagnetism

doi: 10.1093/gji/ggz229

Magnetic mineral assemblage as a potential indicator of depositional environment in gas-bearing Silurian shales from Northern Poland

D. K. Niezabitowska [1], R. Szaniawski [1] and M. Jackson [2]

[1] *Institute of Geophysics Polish Academy of Sciences, Department of Magnetism, Warsaw, Poland. E-mail: dominika.niezabitowska@gmail.com*
[2] *Institute for Rock Magnetism, University of Minnesota, MN, USA*

Accepted 2019 May 17. Received 2019 May 14; in original form 2018 December 7

SUMMARY

Organic matter preservation and associated conditions during deposition, important in the context of fossil fuel exploration, are commonly determined by advanced geochemical analyses. However, the relation between organic matter preservation and magnetic mineral composition remains poorly constrained. The aim of the studies was to check the potential of magnetic mineral differentiation between facies containing various amounts of organic matter as a factor to better understand the processes which influence water chemistry at the bottom of sedimentary basins, and thus to better understand factors controlling the preservation of organic matter. To determine the composition and the properties of magnetic minerals, detailed low-temperature measurements of Saturation Isothermal Remanent Magnetization and hysteresis loops were performed on two types of rocks, Silurian shales from the Baltic Basin (northern Poland). The analysed shale facies are characterized by similar thermal evolution, but different amounts of organic matter: the Pelplin Formation, containing a modest content of organic matter, in which we also examined early diagenetic carbon concretions; and the Jantar Formation, which represents an organic-rich 'sweet spot' layer. In both facies, the results indicate the presence of multi- or pseudo-single domain magnetite, which is interpreted as detrital in origin. However, the main observation gained from this study is the relation between magnetic mineral assemblage in the studied shales and the amount of organic matter: in the rocks with modest amounts of organic matter we observed hematite, while in organic-rich layers hematite was absent. Hematite (mostly single-domain grains) preserved in the Pelplin Formation suggests that stable oxygen-rich conditions were present at the bottom of the sedimentary basin continuously during deposition, concretion cementation and compaction. In turn, its absence in the Jantar Formation suggests that during sedimentation and early diagenesis more anoxic conditions appeared. Generally, findings show that the presence of hematite is related to the significantly lower amount of organic matter in sedimentary rocks. Thus, presence of this mineral may be a useful indicator of organic matter preservation.

Key words: Magnetic properties; Europe; Magnetic mineralogy and petrology; Rock and mineral magnetism; Sedimentary basin processes.

1 INTRODUCTION

The complexity of depositional environments at the bottom of sedimentary basins requires using several different indicators in order to understand the mechanism of the preservation of organic matter, and thus the occurrence of oil and gas in shale rocks. We can list here indicators such as the degree of oxygenation, the degree of bioturbation, the presence of benthic fauna, the salinity (e.g. Rhoads & Morse 1971; Raiswell *et al.* 1988; Calvert & Pedersen 1993; Sageman *et al.* 2003), as well as geochemical characteristics using stable isotopes, biomarkers and trace elements (e.g. Meyers *et al.* 2005; Arnaboldi & Meyers 2007; Algeo & Lyons 2006; Trabucho-Alexandre *et al.* 2012; Goldberg & Humayun 2016). Rock magnetic properties of gas-bearing shale rocks have been also investigated, but mostly in terms of their thermal maturation (e.g. Kars *et al.* 2015; Manning & Elmore 2015).

Our goal was to determine the composition and the properties of magnetic minerals in two shale rock facies characterized by similar thermal evolution, but different amounts of organic matter, and also to define the rock-magnetic differences between them, if any. Next, we intend to evaluate the potential of this differentiation as a factor to better understand the processes which influence water chemistry

at the bottom of sedimentary basins, and thus to better understand factors controlling the preservation of organic matter.

We compared magnetic properties of two kinds of Silurian mudstones: the Pelplin Formation, containing a modest content of organic matter; and the Jantar Formation, which represents the organic-rich 'sweet spot' layer, the most prospective layer of unconventional gas in Northern Poland (e.g. Grotek 1999; Tari *et al.* 2012; Karcz *et al.* 2013). The results of basic rock magnetic measurements from our previous studies (focused on magnetic anisotropy), provided us a general concept of the magnetic mineral assemblage in samples from the Pelplin Formation (Niezabitowska *et al.* 2019). Accordingly, the presence of such minerals as magnetite, probably titanomagnetite or greigite and maghemite was discussed. In this study, in order to fully recognize the magnetic mineralogy in the Pelplin Formation and to determine the presence of magnetic nanoparticles, additional rock magnetic measurements were investigated. In particular, detailed measurements were performed in the temperature range 300–10 K, including changes in SIRM and hysteresis loops with temperature. This kind of analysis provides additional information about magnetic nanoparticles in order to fully recognize the composition of the magnetic minerals, which were not detectible in previous studies. In the case of the Jantar Formation, which was not studied before, we performed a full range of investigations, including key low temperature analysis.

2 GEOLOGICAL SETTING

The samples were collected from organic-rich marine sediments of Silurian age deposited in the Baltic Basin (BB), which was a sedimentary basin located along western margin of the Baltica palaeocontinent. The sedimentary infilling of the BB now forms an elongated syneclize (Peribaltic Syneclize) lying on the East European Craton (EEC, Fig. 1). Our studies were carried out on the middle (axial) part of this syneclize, where strata lie almost horizontally and show only weak signs of tectonic deformations, indicated by the presence of a joint system of Early Devonian (Lochkovian) age (e.g. Poprawa *et al.* 1999). The analysed Wenlockian shales belong to the Pelplin Shale Formation, while deeper the Jantar Formation is Llandoverian (Fig. 2; Modliński *et al.* 2006).

During the Silurian, Baltica was positioned at a palaeolatitude between the equator and 30°S (e.g. Scotese 2001; Verniers *et al.* 2008; Torsvik *et al.* 2017), and the BB constituted a distal foredeep basin of the Pomeranian Caledonides—the orogen formed as a result of the Eastern Avalonia—Baltica collision. The progressive propagation of the Caledonian orogenic front was the main determinant of subsidence associated with flexural bending (after Poprawa *et al.* 1999; Poprawa 2010). The Caledonian front and associated accretionary prism were also a source of detrital material deposited in the BB during Silurian (Jaworowski 2002; Modliński & Podhalańska 2010 and earlier papers). However, the significant abundance of carbonates in the analysed rocks may suggest a secondary source of detrital material—an eastward carbonate platform on the Baltica margin (e.g. Lazauskiene *et al*. 2003, Calner 2005).

The Silurian sediment complex of the present western margin of the EEC shows variable thermal alteration levels. According to the results of Karcz *et al.* (2013) and Caricchi *et al.* (2015) on analysed drill cores from the Silurian shales of the BB, in the depth interval 2400–4300 m the values of Ro (vitrinite reflectance) do not exceed 1.42 per cent. These values imply that the Silurian sediments are in the early dry gas generation stage, up to the wet gas generation stage of diagenesis/catagenesis (Mastalerz *et al.* 2013). This maximum burial stage, corresponding to a maximum palaeotemperature of 150 °C, occurred before the end of Devonian time (e.g. Grotek 1999; Środoń & Clauer 2001).

Despite the large amount of total organic carbon (TOC) data for the Peribaltic Syneclize (e.g. Zdanavičiūtė & Lazauskienė 2009; Kowalski *et al.* 2010), detailed information about the distribution of organic matter in each of the Silurian intervals is poorly recognized. Most of the studies were focused on defining the petroleum potential of the Palaeozoic strata in the Polish part of the Baltic region, and thus to examine the TOC content and type of organic matter. In the individual boreholes the Silurian strata are locally enriched in organic matter, while the present TOC content reaches locally 10 wt. per cent (usually 1–2 wt. per cent, Kowalski op. cit.).

3 SAMPLES AND METHODS

The samples come from two homogenous lithofacies from two shale gas exploration wells (labelled A and B) located in Northern Poland, which were derived by the Polish Oil and Gas Company. The samples JAN1–3 represent the most prospective (in the context of gas exploration) shale layer, called the Jantar Formation, where TOC reached 5 per cent (Karcz *et al.* 2013). Samples JAN1–3 were collected from depths of 3670 m (drill core A) and 3940 m (drill core B). The second type of samples (PEL1–3) represent mudstones from the middle part of the Pelplin formation, which contain smaller amounts of TOC (not exceeding 1.5 per cent) and are characterized by the presence of calcareous concretions. The depths of collected samples of the Pelplin Formation are approximately 3595 m for drill core A and 3825 m for B.

Samples were collected also from the calcareous concretions, which occur in the Pelplin shales, from the same depth intervals as the mudstone samples (Fig. 2). Those concretions were cemented during the early stage of diagenesis, before the end of compaction of the surrounding mudstones (Niezabitowska *et al.* 2019), so the record of primary geochemical conditions from the period of the early stage of sediment deposition and compaction is expected to be preserved in them (compare with Day-Stirrat *et al.* 2008).

3.1 Rock magnetic studies on the Jantar Formation at room and high temperatures

These experiments were performed at the Palaeomagnetic Laboratory of the Institute of Geophysics, Polish Academy of Sciences, Warsaw, Poland.

To constrain the magnetic mineralogy the measurements were initiated by acquisition of Isothermal Remanent Magnetization (IRM) experiments. Six specimens of 26/22 mm in size (diameter/length) were magnetized using eight steps up to 3 T in an MMPM1 pulse magnetizer and measured at each magnetization step using a 2 G SQUID (the USA) cryogenic magnetometer (noise level $\sim 10^{-10}$ Am^2).

The temperature variation of magnetic susceptibility in air was measured on eight powder samples with a Kappabridge KLY-3S [AGICO, Czech Rep., sensitivity 2×10^{-8} (SI), accuracy 0.3 per cent]. To estimate the percentage contribution of ferro- and paramagnetic minerals to the total susceptibility of the samples, the method of Hrouda (1994) and Hrouda *et al.* (1997) was applied, through fitting a hyperbola to the initial part of a thermomagnetic curve (the 50–250 °C temperature range), using the least-squares method. The calculations were conducted in Cureval8 software (AGICO).

To better establish the magnetic properties of these rocks, and in particular the ferro/paramagnetic content, hysteresis loops were measured using a Vibrating-sample Magnetometer (Micro-Mag Princeton Measurements Corp., USA, noise level $\sim 10^{-7}$ Am^2) on small rock chips (not exceeding 0.02 g). Four samples from a facies per each drill core were analysed. The paramagnetic slope correction was applied by the standard MicroMag AGM software correction.

3.2 Low temperature remanence

The measurements at low temperatures were investigated at the Institute for Rock Magnetism, University of Minnesota, Minneapolis, USA. The measurements were conducted using Magnetic Properties Measurement System instruments (MPMSs, built by Quantum Design Inc., San Diego). All measurements were done on fifteen powder samples (not exceeding 400 mg), enclosed in gel capsules.

These measurements start with applying a 2.5 T field at room temperature to reach SIRM (Saturation Isothermal Remanent Magnetization). The next step was to cool down the sample from 300 to 10 K (26.85 to –263.15 °C) in a weak magnetic field (5 μT), in 5 K steps. This part of the measurements is called Room Temperature SIRM (RT-SIRM) cooling. In general, the SIRM measurement as a function of temperature is performed in zero magnetic field. However, based on Aubourg & Pozzi (2010), as well as Kars *et al.*

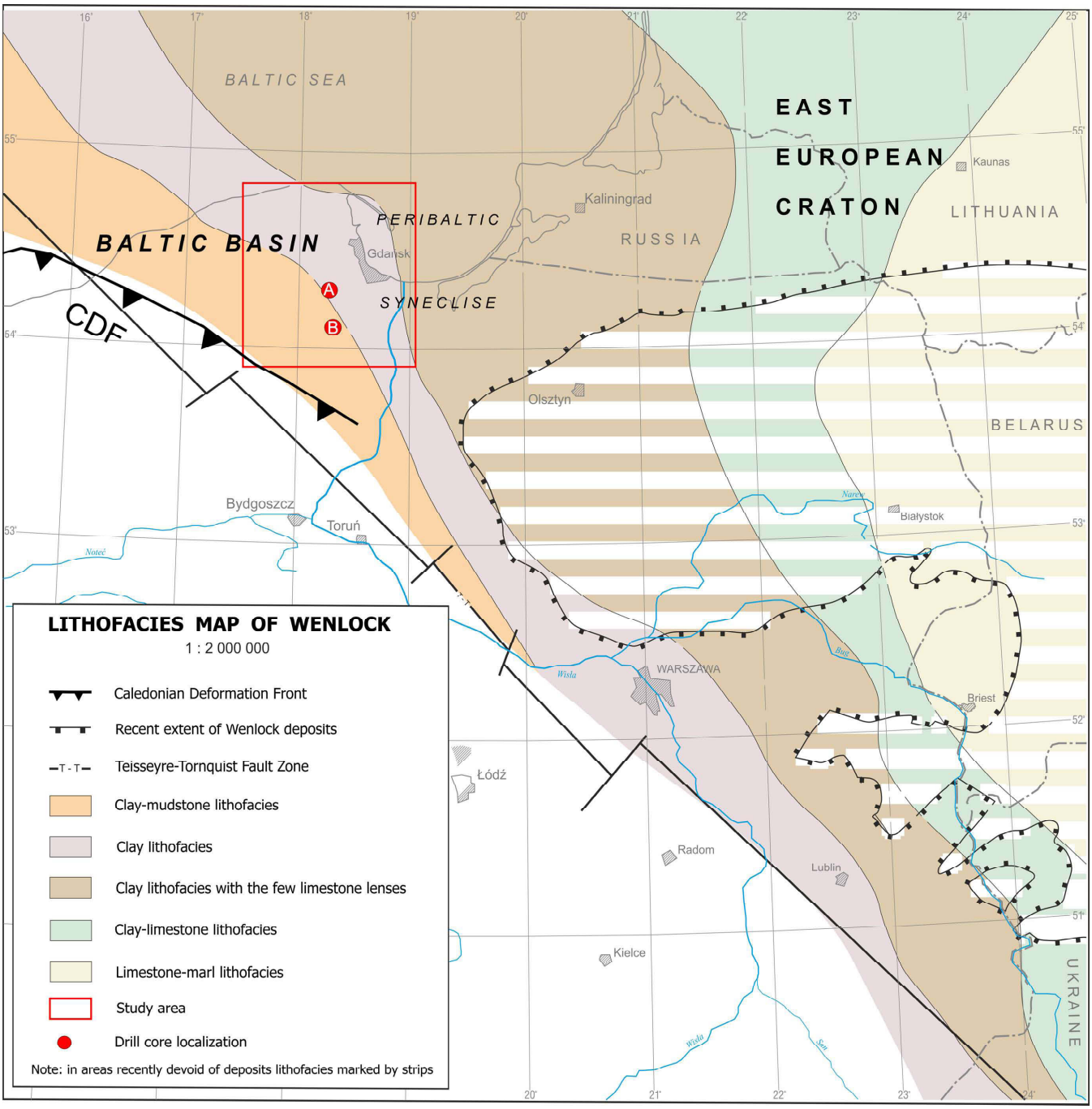

Figure 1. Simplified lithofacies map of Wenlock in the NE Poland (after Modliński 1976, simplified and modified) with the study area in the red rectangle. CDF, Caledonian Deformation Front (after Grad *et al.* 2002).

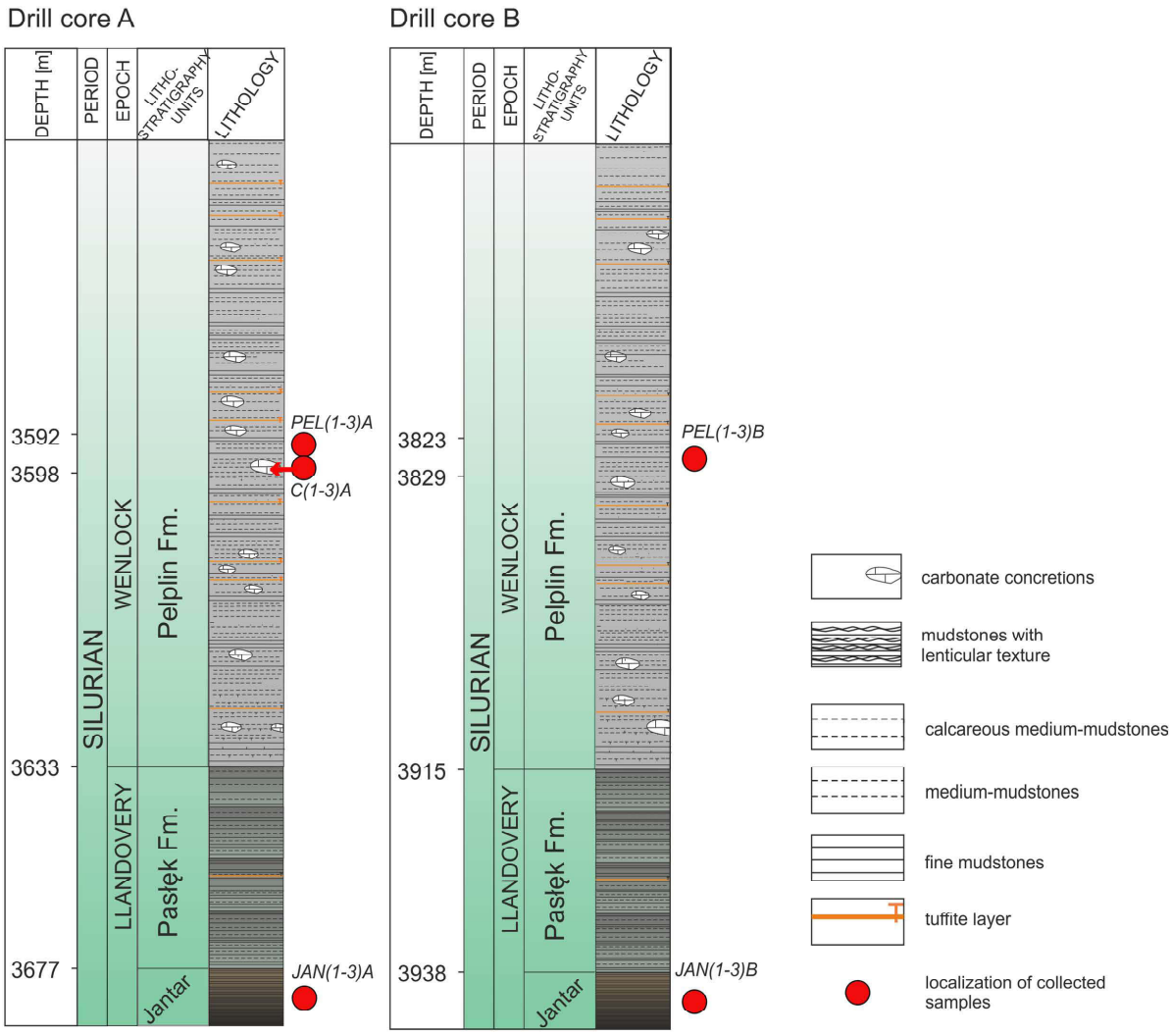

Figure 2. Lithostratigraphic profiles of Silurian rocks from Pomerania region from two shale gas exploration wells (A and B). Samples came from the Jantar and Pelplin formations.

(2014; 2015), a 5 μT field was applied to intensify the so-called P-behaviour, which was originally proposed as a diagnostic indicator of nano-pyrrhotite (Aubourg & Pozzi 2010) but is now thought to be determined primarily by the occurrence of paramagnetic minerals (Kars & Aubourg 2014, 2015). These RT-SIRM cooling experiments in a small (5 μT) magnetic field represent a combination of remanent and induced magnetizations (and the measurement curves are labelled as 'other' in the plots to follow). The next step was to apply a 2.5 T field at 10 K (–263.15 °C) to reach LT-SIRM (low temperature SIRM). After switching off the magnetic field, the sample was warmed up to 300 K (26.85 °C) in zero field (ZF) in 10 K steps.

A more comprehensive measurement sequence comprises the two preceding steps and additional steps to evaluate the effects of cooling in a strong field (field cooling, FC) and to observe the recovery of RT-SIRM on rewarming in ZF. This set involves: (1) FC in 2.5 T to 10 K (–263.15 °C); (2) measurement while warming to room temperature in ZF; (3) cooling to 10 K (–263.15 °C) in ZF; (4) measurement while warming to 300 K (26.85 °C) in ZF; (5) imparting a 2.5 T RT-SIRM; (6) measurement while cooling to low temperature in ZF and (7) measurement while rewarming to room temperature in ZF.

3.3 Hysteresis loops at low temperatures

The hysteresis loops were performed on a Princeton Measurements Vibrating Sample Magnetometer (sensitivity 5×10^{-9} Am^2). The loops were measured in steps of increasing temperature from 10 to 300 K to determine the magnetic property changes related to mineral composition, which result in different shapes of the ZFC curves (see details in Figs 5C and D). Two samples (JAN1 and JAN3 from the 'sweet spot' formation) were comprehensively measured. The hysteresis loops (2.5 T field maximum) were measured at the following temperatures: 10, 20, 50, 90, 150 and 300 K (–263.15, –253.15, –223.15, –183.15, –123.15 and 26.85 °C, respectively). The measurements were performed on powder samples (not exceeding 400 mg) enclosed in gel capsules.

4 RESULTS AND INTERPRETATION

Previous investigations on the Pelplin Formation show that magnetic susceptibility is controlled by paramagnetic minerals, most likely phyllosilicates (represented by chlorite, illite and smectite), which constitute approximately 50 per cent of the mineral composition of the mudstones and 35 per cent in calcareous concretions, and also partially by pyrite, which is present in significant amounts

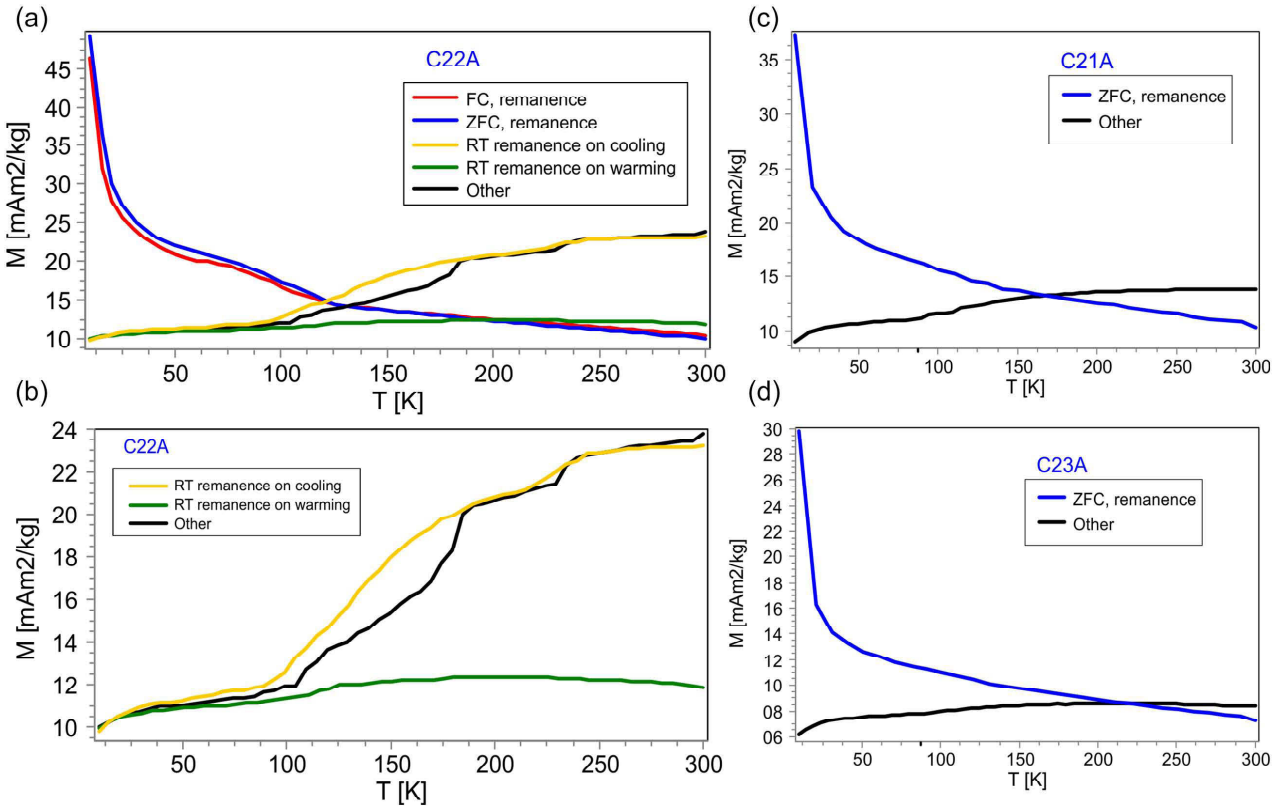

Figure 5. The results of MPMS measurements of remanence in low temperature range (10–300 K; –263.15 to 26.85 °C) for selected samples of calcareous concretions from the Pelplin Formation. (a) ZFC and FC remanence, RT-SIRM while cooling and warming, and 'Other' curve; (b) RT-SIRM while cooling and warming, and 'Other' curve; (c) ZFC and 'Other' curve; (d) ZFC and 'Other' curve. ZFC, Zero Field Cooled; FC, Field Cooled (FC). Room Temperature SIRM, the 'Other' curves are RT-SIRM measured while cooling in a small (+ 5μT) applied magnetic field.

(Niezabitowska *et al.* 2019). Moreover, the presence of clearly predominant low-titanium magnetite, maghemite (in carbonate concretions), and probably titanomagnetite/greigite was determined, while slight signs of high coercivity minerals, like hematite or goethite were detected after applying the IRM acquisition curve experiments, interpreted by using the method of Kruiver *et al.* (2001), and the thermal demagnetization of three-component IRM (Niezabitowska *et al.* 2019).

4.1 The results of rock magnetic measurements for the Jantar Formation

The results of the IRM acquisition show relatively rapid increasing of the remanence in weak magnetic fields (below 0.3 T), which is typical for rocks dominated by low-coercivity minerals (e.g. ferrimagnetic magnetite or maghemite). In the range between 0.3 and 0.75 T a continued slow increase is visible, suggesting the presence of some medium coercivity minerals. Saturation of the IRM after applying 1 T field does not indicate the presence of high coercivity minerals (e.g. imperfectly antiferromagnetic hematite or goethite; Fig. 3A).

To determine the contribution of ferro- and paramagnetic minerals, temperature variation of magnetic susceptibility and hysteresis loops were performed. The beginning of the thermal variation curves displays a hyperbolic shape, which is characteristic of paramagnetic minerals (Fig. 3C). At temperatures over 400 °C, the formation of new magnetic minerals is observed (Fig. 3C). The separation method demonstrates that magnetic susceptibility of unheated samples is mainly controlled by paramagnetic minerals (accounting for 71–94 per cent of the total susceptibility).

These results are in line with the outcomes of hysteresis experiments. In general, the shape of the hysteresis loops indicates the domination of a paramagnetic behaviour (linear and reversible) with a small amount of a ferromagnetic phase (Fig. 3D), which is well marked after correction for a paramagnetic minerals (Fig. 3E). Estimated percentage contribution of ferromagnetic minerals to the low-field susceptibility is in the 7–16 per cent range, and the mass concentration of ferrimagnetic minerals such as magnetite can be estimated from M_s to be on the order of several parts per million (Table 1).

4.2 Low temperature measurements

The samples from the Pelplin Formation display well defined Verwey transitions, indicative of magnetite, on the RT-SIRM curves (Figs 4B and D), while in both ZFC and FC curves the transition is hardly visible (Figs 4A and C), which may suggest titanium substitution or a grain size effect (for further discussion see 5.1.). This transition occurs at ∼110–115 K [–163.15 to (–158.15) °C], slightly below the transition temperature for pure stoichiometric magnetite, indicating a small degree of cation deficiency. For this formation the Morin transition of hematite is also well marked and occurs at ∼220–240 K [–53.15 to (–33.15) °C] on the RT-SIRM curves (Fig. 4B). Values of ZFC remanence slightly higher than those of FC remanence (Fig. 4A) indicate that the magnetite may be a mixture of single domain (SD) and multidomain (MD) grain sizes or

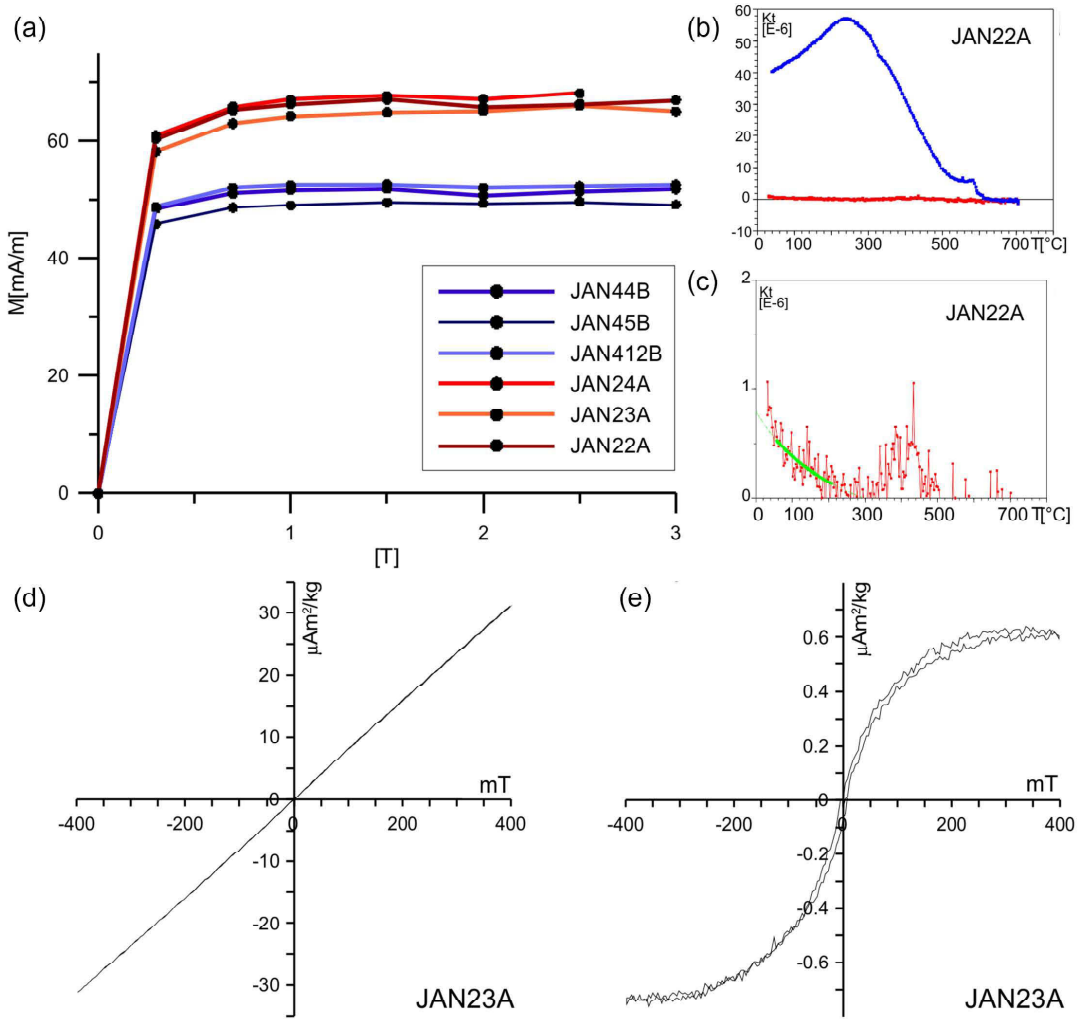

Figure 3. The results of IRM acquisition (a), curves of thermal variation of magnetic susceptibility: red curve—heating, blue curve—cooling, green curve—fitted hyperbola (b, c) and hysteresis loops before (d) and after automatic correction for paramagnetic minerals (e) for selected specimens from the Jantar Formation.

Table 1. Hysteresis loop parameters for selected samples of the Jantar Formation with calculation of ferro- and paramagnetic contribution.

	SAMPLE	M_s (μAm^2 kg^{-1})	M_r (μAm^2 kg^{-1})	B_c (mT)	Ferromagnetic contribution (per cent)
DRILL CORE A	JANA_21	670.5	36	5.88	7.18
	JANA_22	635.5	40.56	5.83	7.27
	JANA_23	530.4	38.31	6.48	6.55
	JANA_24	554.3	35.37	6.34	7.28
DRILL CORE B	JANB_11	435.6	37.6	8.07	16.41
	JANB_12	476.4	35.93	8.35	10.91
	JANB_13	663.5	56.12	6.30	14.58
	JANB_14	503.5	46.11	8.07	12.12

Note: M_s, saturation magnetization after correction for paramagnetic minerals; M_r, magnetic remanence; B_c, coercivity. Ferromagnetic contribution is calculated from initial slope after (ferromagnetic susceptibility) and before correction for paramagnetic minerals (total susceptibility).

may be primarily in the intermediate pseudo-single domain (PSD) size range. These are consistent with relatively low recovery of RT-SIRM remanence curve during heating (Fig. 4B; Carter-Stiglitz *et al.* 2006).

Similar results were obtained for calcareous concretions from the Pelplin Formation. The Verwey transition is well developed on RT-SIRM curves (Figs 5A and B). In contrast to the mudstones, the transition is also clearly visible in both the ZFC and FC curves (Fig. 5A, compare Table 2). For these rocks the Morin transition of hematite is also well marked and occurs at ∼230–240 K [–43.15 to (–33.15) °C] on the RT-SIRM curves (Figs 5A and B). Similarly, like in the mudstones, slightly higher values of ZFC than FC remanence are visible, suggesting the presence of PSD and/or a mixture of SD and MD grains (Fig. 5A; see Jackson *et al.* 2011). This again corresponds with relatively low recovery of magnetization on RT remanence curve during heating (Fig. 5B; Carter-Stiglitz *et al.* 2006). Note that the difference between the 'other' curve (cooling

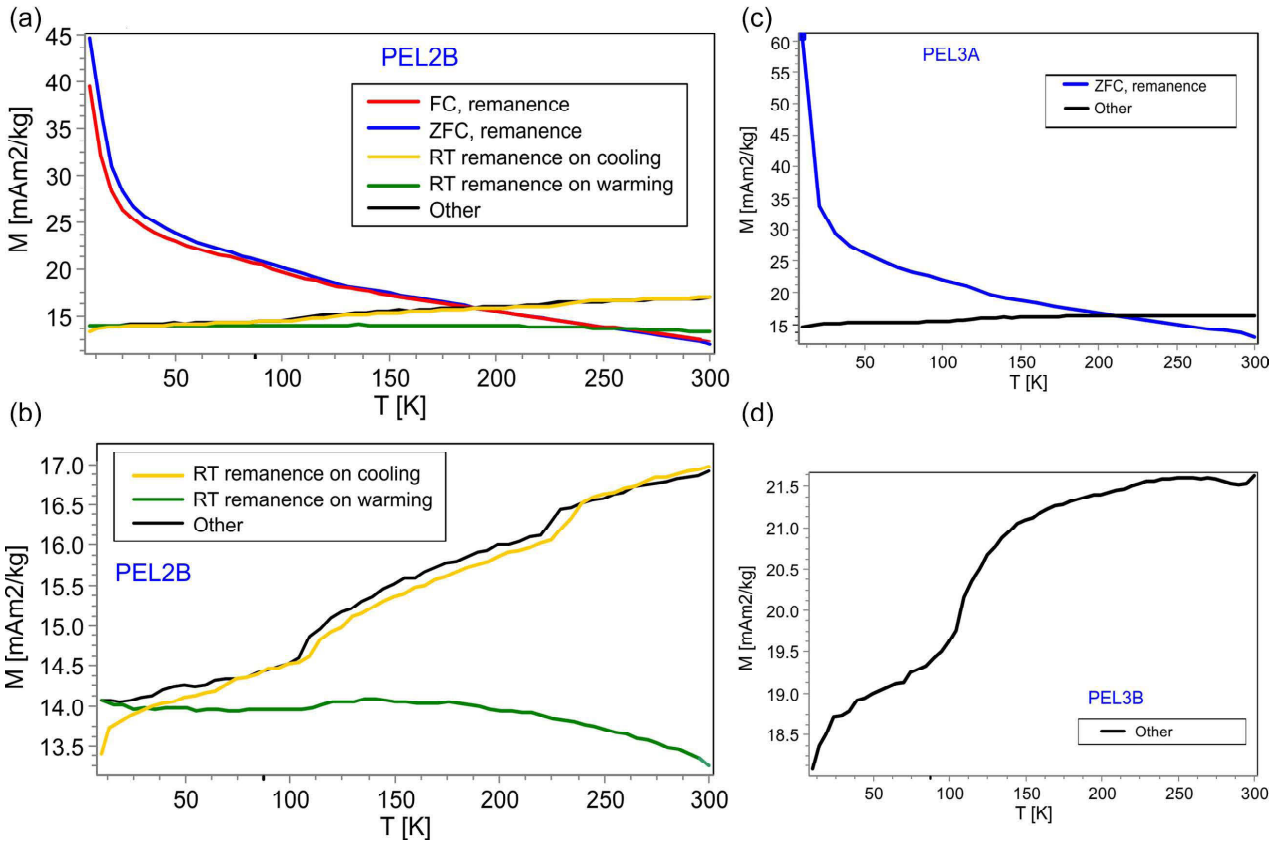

Figure 4. The results of MPMS measurements of remanence in low temperature range (10–300 K; –263.15 to 26.85 °C) for selected samples from the Pelplin Formation: (a) ZFC and FC remanence, RT-SIRM while cooling and warming, and 'Other' curve; (b) RT-SIRM while cooling and warming, and 'Other' curve; (c) ZFC and 'Other' curve and (d) 'Other' curve. ZFC, Zero Field Cooled; FC, Field Cooled. Room Temperature SIRM; the 'Other' curves are measurements of the RT-SIRM while cooling in a small (+5 μT) applied magnetic field.

Table 2. Summarized results of magnetic minerals composition for each formation.

Formation	Lithology	Transition temperature [K]	Magnetic mineral	Particles		
				MD/PSD	SD	SP
Pelplin	mudstones	110–115	magnetite	×	× ?	×?
		220–240	hematite	×?	×	
	calcareous	110	magnetite	×	×?	×?
	concretions	230–240	hematite	×?	×	
Jantar	mudstones	120	magnetite	×		

Note: ×, presence; ×?, probable occurrence, see details in Discussion.

Table 3. Results of Field Cooled (FC) hysteresis loops for two selected samples from the Jantar Formation.

Sample	T [K]	M_s [Am^2/kg]	M_r [Am^2/kg]	B_c [mT]	χ_{hf} [m^3/kg]	Q	Q_f
JAN3B	10	3.61E-01	1.97E-04	0.151	5.89E-07	2.3	2.09
	20	4.80E-01	1.53E-04	0.917	3.37E-07	2.19	2.49
	50	1.28E-02	1.48E-04	1.623	2.10E-07	3.17	2.44
	90	5.75E-03	1.62E-04	4.163	1.09E-07	3.01	2.05
	150	6.90E-03	1.80E-04	3.981	6.04E-08	3.28	2.53
	300	5.12E-03	2.50E-04	6.119	2.69E-08	3.05	2.39
JAN1A	10	5.72E-01	-2.85E-03	1.698	1.01E-06	2.44	2.2
	20	2.65E-01	-6.81E-04	-0.218	7.59E-07	2.68	2.41
	50	5.99E-03	-1.61E-04	-6.603	3.70E-07	3.16	1.33
	90	1.42E-03	-7.28E-05	62.144	1.88E-07	2.76	1

T, temperature; M_s, saturation magnetization; M_r, magnetic remanence; B_c, coercivity; χhf, high field susceptibility; Q, data quality; Q_f, quality factor for the ferromagnetic loop (obtained by correction for the linear high-field slope). Temperatures as follow: 10, 20, 50, 90, 150 and 300 K (–263.15, –253.15, –223.15, –183.15, –123.15 and 26.85 °C, respectively).

of the RT-SIRM in a small applied magnetic field) and zero-field RT-SIRM cooling curve is most probably connected with reorientation of sample grains during measurement.

The samples from the Jantar Formation display very well developed Verwey transitions on the RT-SIRM cooling curves (Figs 6B, D and E), which is also clearly visible in both the ZFC and FC warming curves (Figs 6A and D). In all specimens the transitions occur at ∼120 K (–153.15 °C), suggesting fairly pure magnetite, and the grain size is probably mainly MD magnetite, due to significant difference in ZFC and FC intensities below T_V (Fig. 6A) and the small recovery of remanence upon rewarming of the RT-SIRM (Fig. 6B; Carter-Stiglitz *et al.* 2006). In contrast to the Pelplin Formation, the lack of the Morin transition suggests that this facies does not contain hematite.

Generally, in all samples, both from the Jantar and Pelplin formations, approximately 50–60 per cent losses of magnetization on the FC and ZFC curves upon warming to 35 K (–238.15 °C, Figs 4, 5 and 6), may suggest (a) unblocking of very small superparamagnetic (SP) or SD particles and/or (b) disordering of phases like siderite or ilmenite with Neel temperatures below 300 K (26.85 °C) and/or (c) decreasing magnetocrystalline anisotropy in phases like goethite (e.g. Banerjee *et al.* 1993; Passier & Dekkers 2002).

The low-temperature hysteresis loops generally had high Q values (2 or greater) indicating good overall data quality, and Q_f values of at least 1, indicating generally acceptable quality of the ferromagnetic loops obtained by subtraction of the calculated paramagnetic component (Table 3., Jackson & Solheid 2010). However, the loops are almost perfectly reversible (i.e. almost no remanence or coercivity), so the remanence-related parameters M_r and B_c are poorly defined (taking on physically unrealistic negative values in some cases), (Fig. 7, Table 3). Clear results were obtained for 300 K and 150 K (26.85 and –123.15 °C), where the contribution of low coercivity minerals is evident. At lower temperatures the magnetization is much more intense, and does not saturate, even in 2.5 T field. The origin of the intense low-T magnetization is somewhat uncertain. It may be due in part to low-temperature magnetic ordering of an iron-bearing phase that is paramagnetic at room temperature. Alternatively, at least some of the strong increase is due to the inverse temperature dependence of paramagnetism, and at these low temperatures and high fields, paramagnetic moments begin to show nonlinear field dependence, which makes it difficult to separate them from hard ferromagnets. We have processed the loops with approach-to-saturation fitting (Jackson & Solheid 2010), and thus the intense, slowly saturating phases are in effect counted as ferromagnetic. Strong increases (more than 90 per cent) of saturation magnetization (M_s) are well marked in the 50–10 K (–213.15 to –263.15 °C) range (Fig. 8A). Similar trend is observed for high field susceptibility (χ_{hf}), where values increase approximately 60 per cent from 50 to 10 K (–213.15 to –263.15 °C) for both samples (Fig. 8B).

5 DISCUSSION

5.1 Magnetite

In all types of rocks, both mudstones and calcareous concretions from the Pelplin Formation as well as mudstones of the Jantar Formation, the Verwey transition is clearly marked on the RT-SIRM curves at temperatures of 110–120 K (–163.15 to –153.15 °C, Figs 4–6). This temperature range is characteristic for nearly stoichiometric magnetite. The lack of recovery on rewarming of the RT-SIRM, and the ratios of ZFC to FC magnetization greater than one, imply that among all of the magnetite grains present in the rock the PSD-MD fraction is dominant. We suppose that these relatively large magnetite grains (μm to tens of μm) are most likely detrital in origin (compare with Chang & Kirschvink 1989; Channell *et al.* 2013; Chang *et al.* 2016).

In calcareous concretions of the Pelplin Formation and in the Jantar mudstones the Verwey transition is clearly defined on both, RT-SIRM and ZFC/FC curves, while in the Pelplin mudstones the transition is apparent only on the RT-SIRM cooling curve (compare Figs 4–6). In all cases, the transition is not sharp, but spread out over a temperature interval of ten degrees or more. The suppression or masking of the Verwey transition in the Pelplin warming curves can be explained by a variety of factors, such as non-stoichiometry and/or cation substitution in magnetite crystals or grain size effects (e.g. Syono 1965; Aragón *et al.* 1985; Kąkol & Honig 1989; Kąkol *et al.* 1992; Moskowitz *et al.* 1993; Özdemir *et al.* 1993; Halgedahl & Jarrard 1995; Moskowitz *et al.* 1998). In the ZFC/FC curves, unblocking of SD-SP grains and/or demagnetization of phases like goethite cause continuous loss of remanence over wide ranges of temperature, which may obscure the evidence of the Verwey transition, especially when it is not sharp (e.g. Liu *et al.* 2003). Therefore, we suggest that in mudstones of the Pelplin Formation, where no evidence of goethite was found, the SD-SP particles appearance or nonstoichiometry might account for the lack of a clearly observed Verwey transition.

We note that in general the best way to document the presence of SP populations is through low-temperature frequency-dependent susceptibility [$\chi(f,T)$] measurements, but these samples were not suitable for $\chi(f,T)$ analysis, because of the very high ratio of paramagnetic/ferromagnetic susceptibility. Nevertheless the remanence curves strongly suggest the presence of such magnetic nanoparticles. There are several models explaining the origin of the SP-SD particles in sedimentary rocks. They may be formed as a product of reductive dissolution of PSD and MD detrital magnetite (Karlin & Levi 1983; Tarduno 1995; Smirnov & Tarduno 2001) or an oxidation of preexisting iron sulfides nanoparticles in suboxic layer (e.g. Tarduno 1995). Furthermore, magnetotactic bacteria can be also taken into account as a possible source of natural magnetite nanoparticles (e.g. Kirschvink & Chang 1984; Petersen *et al.* 1986; Chang & Kirschvink 1989).

However, due to the abundance of clay minerals in the analysed mudstones (approximately 50 per cent), including an abundance of illite-smectite mixed layers (Środoń & Clauer 2001), neoformed ferromagnetic grains may have appeared mainly as a result of smectite illitization and pressure solution (Katz *et al.* 2000; Woods *et al.* 2002; Zegers *et al.* 2003; Oliva-Urcia *et al.* 2008). This model may be supported by the diagenetic ages of fine fractions of Silurian shales described by Środoń & Clauer (2001). On the other hand, the significant amount of organic matter suggests that the origin of the SD-SP particles might also be related to the maturation of organic matter as in models proposed by Lovley *et al.* (1987) or Blumstein *et al.* (2004). Nevertheless, these processes, illitization and/or maturation, are even more likely to have occurred in the deeper Jantar Formation, where mixed phyllosilicates and an abundance of organic matter are present. Thus, we can infer that the lack of a visible Verwey transition in the Pelplin warming curves is not primarily due to the presence of an overwhelming SP decay in those samples.

Therefore, to explain the suppression of the Verwey transition in the Pelplin mudstones we should focus on: (1) magnetite non-stoichiometry or (2) chemical and redox conditions responsible

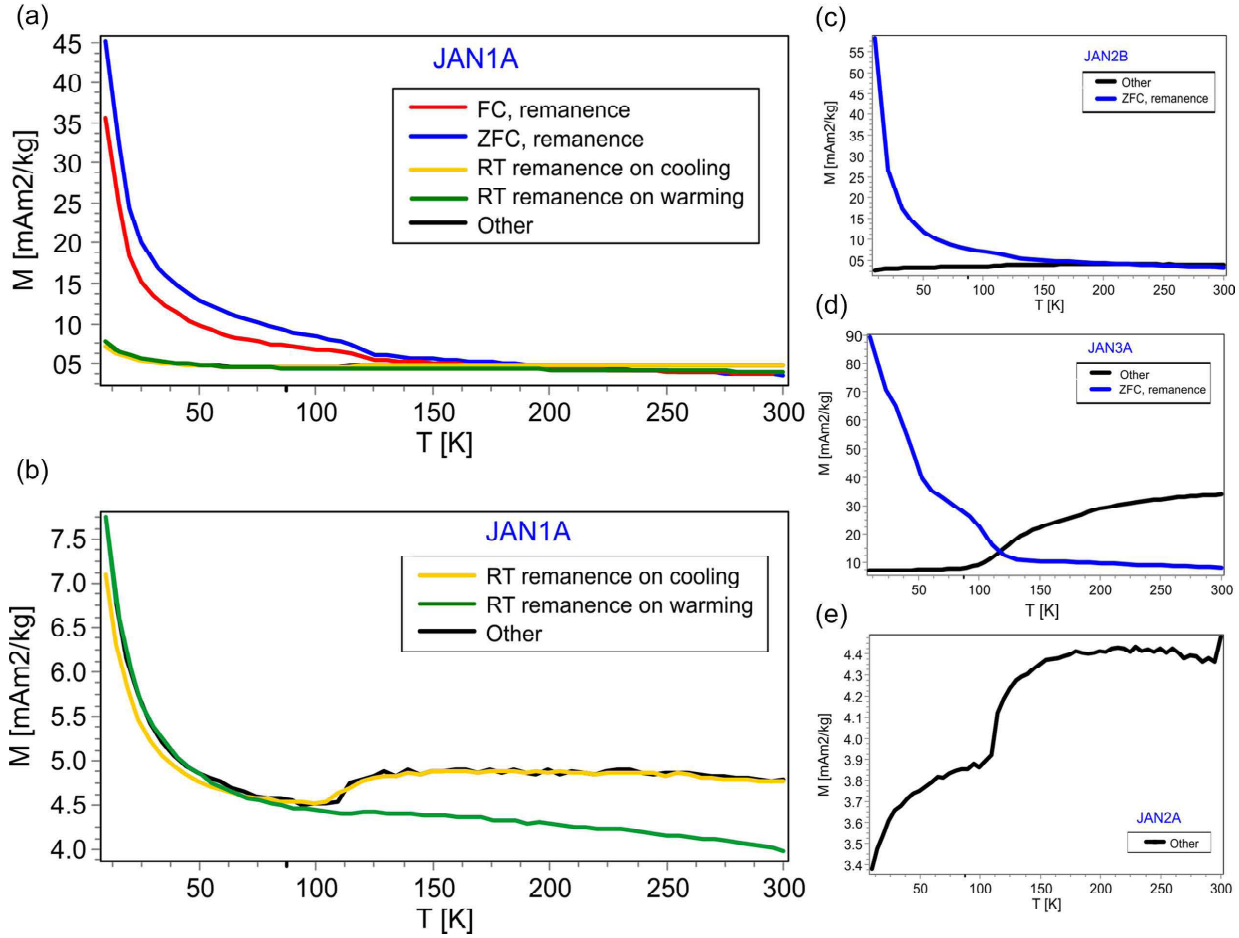

Figure 6. The results of low temperature remanence for selected samples from the Jantar Formation: (a) ZFC and FC remanence, RT-SIRM while cooling and warming, and 'Other' curve; (b) RT-SIRM while cooling and warming, and 'Other' curve; (c) ZFC and 'Other' curve; (d) ZFC and 'Other' curve; (e) 'Other' curve. Abbreviations: Zero Field Cooled (ZFC), Field Cooled (FC), Room Temperature SIRM, the 'Other' curves are RT-SIRM measurements while cooling a small (+5 μT) applied magnetic field.

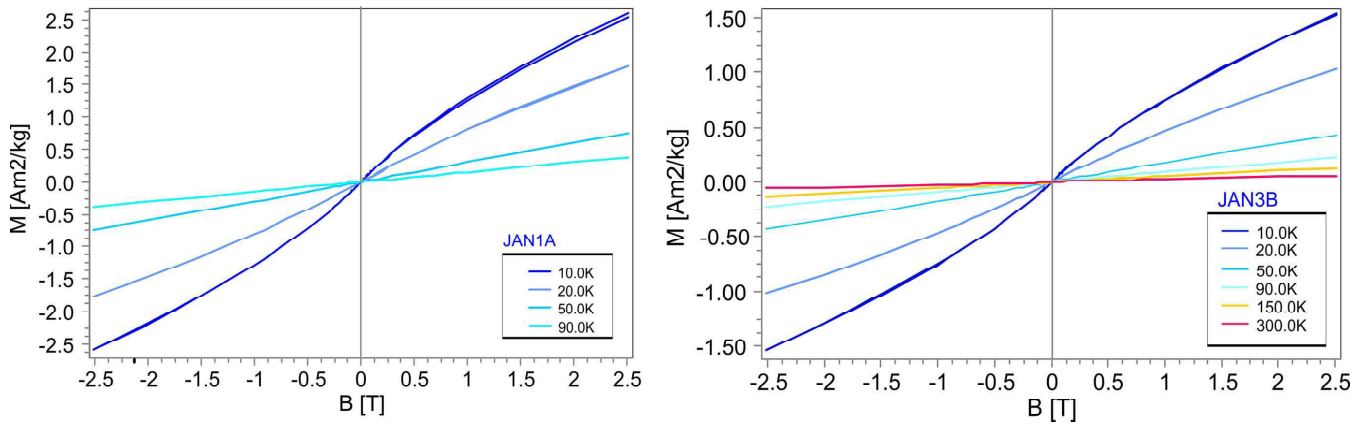

Figure 7. Low-temperature hysteresis loops in the 300–10 K (–263.15 to 26.85 °C) temperature range for two selected samples from the Jantar Formation.

for the appearance of neoformed minerals. The magnetite nonstoichiometry might be connected with either cation deficiency due to low-temperature oxidation (e.g. Ozdemir *et al.* 1993; Ozdemir & Dunlop 2010; Chang et al 2013), or cation substitution, mainly the presence of titanium in detrital Fe–Ti oxides (Morad & Aldahan 1986; Roberts & Turner 1993). The presence of carbonate concretions in the Pelplin Formation helps to understand the complex processes and depositional conditions during sediments accumulation.

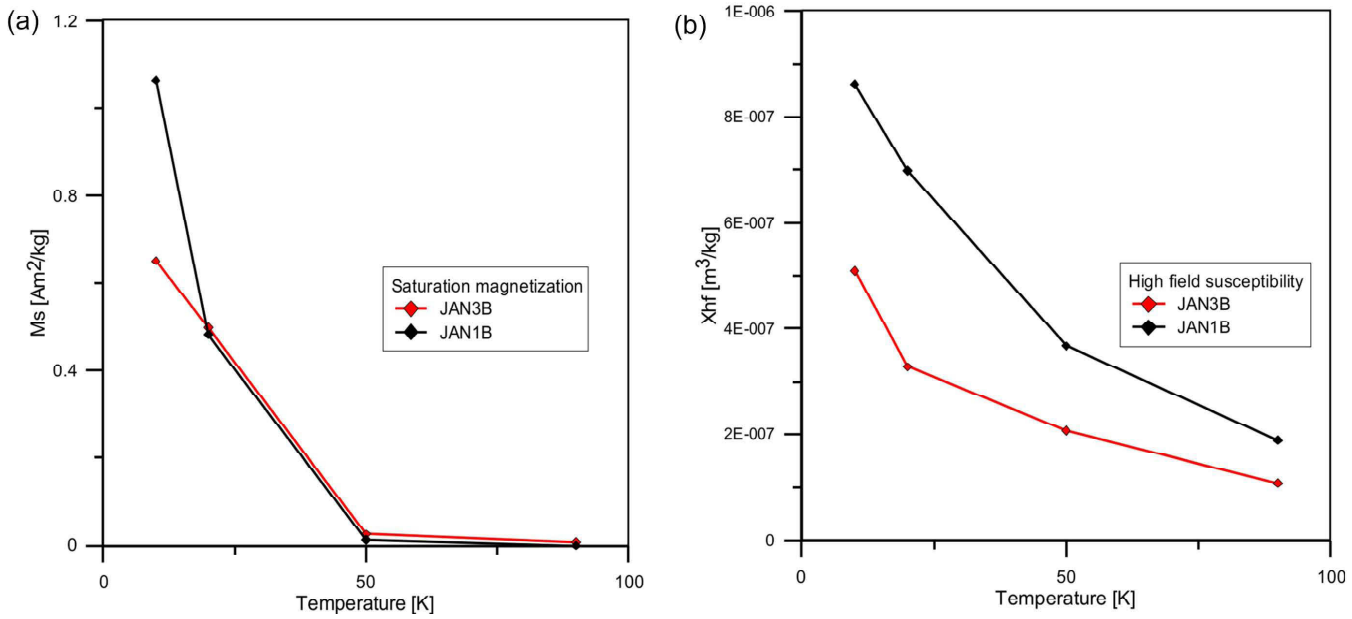

Figure 8. Evolution of saturation magnetization (a) and high field susceptibility (b) from 10 K to 90 K (–263.15 to –183.15 °C) for two selected samples from the Jantar Formation.

5.2 Hematite

In contrast to the Jantar Formation, in the Pelplin Formation the occurrence of hematite (see Figs 4 and 5), is observed in both mudstones and calcareous concretions. According to Özdemir *et al.* (2008) the Morin transition at approximately 220–240 K (–53.15 to –33.15 °C) may suggest grain size of the hematite about 0.04–0.1 μm in diameter. Thus, this size of grains corresponds with SD like behaviour (Kletetschka & Wasilewski 2002). Lower temperatures of the Morin transition [approximately 230 K (–43.15 °C), Fig. 2b] can be explained by reduction of grain size, crystal morphology or substitutions (Özdemir *et al.* 2008).

Current models explaining the presence of hematite in deep marine sediments suggest a detrital origin, involving aeolian processes (e.g. Balsam *et al.* 2007; Channell *et al.* 2013), hyperpycnal flood events or turbidity currents (e.g. Uhlein *et al.* 2011; Labuhn *et al.* 2018). Hematite in hemipelagic environments may be also formed as a product of a magnetite reaction in oxygenic waters during sedimentation (e.g. Murray 1979; Chang & Kirschvink 1989) or it can be preserved as hemo-ilmenite domains in sediments derived from silicic volcanic rocks (e.g. Nord & Lawson 1989; Roberts & Pillans 1993; Roberts & Turner 1993; Kiipli *et al.* 2000; Kiipli 2004). However, an origin of hematite related to the metabolic pathway of Fe-oxidizing bacteria in oxic/suboxic conditions is also possible (Chang & Kirschvink 1989; Edwards *et al.* 2012; Hatfield 2014).

Considering the size of the detected hematite grains in the analysed Pelplin rocks we can suppose that the most probable scenario for hematite is a detrital origin, likely by aeolian transport of material. On the other hand, the frequent occurrence of tuffite layers in the Pelplin Formation (see Fig. 2) might suggest that hematite was formed in situ under the influence of chemical changes, not continentally derived, like in models proposed by Kiipli (2004).

Generally, the circumstances to preserve hematite in depth of 100s m during sedimentation favour oxic to suboxic conditions (Liu *et al.* 2004; Roberts & Weaver 2005), and also low sedimentation rate (e.g. Kiipli 2004), which is linked with decreasing aerobic and anaerobic degradation of organic matter (Tromp *et al.* 1995). In the Pelplin Formation we observed a higher sedimentation rate than in the lower Jantar Formation, which occurred due to the approaching CDF. Despite this fact, more oxygen-rich conditions appeared, which led to a reduction of organic matter in this facies and at the same time led to preservation of hematite. In turn, an absence of hematite in the organic-rich Jantar Formation can be linked with rather anoxic conditions at the bottom and with very low sedimentation rate (see Karlin & Levi 1983; Karlin & Levi 1985 for discussion).

An interesting conclusion comes from the presence of calcareous concretions in the Pelplin Formation, whose precipitation is commonly linked with suboxic conditions (for discussion see Lash & Blood, 2004; Lash, 2015). Overall, the calcareous concretions were formed as a result of cementation during the early stages of diagenesis and they have been preserved as rigid bodies. Thus, as resistant to deformations and diagenesis, they are predisposed to preserve the record of early diagenetic geochemical conditions (e.g. Day-Stirrat *et al.* 2008). This fact suggests that chemical conditions during deposition and compaction of detrital material of the Pelplin Formation, and continuously during precipitation of the carbonate concretions, were relatively stable and oxic, and also that the hematite appeared in the very early stage of diagenesis. To conclude, this finding does not clearly show the source of hematite, but in our opinion it may have a detrital as well as early diagenetic origin; in any case, it certainly appeared in the very early stage of the rock overgrowth.

In the Jantar Formation, higher TOC (up to 5 per cent) and absence of hematite are detected, while in the Pelplin Formation hematite and lower TOC values (not exceeding 1.5 per cent) are documented. The occurrence of the hematite in the Pelplin Formation (Wenlock) and its absence in the deeper layer of the Jantar Formation (Llandovery) can be associated with variations of oxidation conditions in the sedimentary basin during *ca*. 10 Ma, as in the results of Kiipli (2004) and Vanderbroucke *et al.* (2013).

Several factors control oxidation conditions at the bottom of the sedimentary basin, and directly influence the preservation of organic matter, such as sedimentation rate, subsidence/uplift, sea level and variations in primary marine productivity or amount of delivered

detritus (e.g. Froelich *et al.* 1979; Wilson *et al.* 1986; Schulz *et al.* 1994; Meyers & Shaw 1996; Vanderbroucke *et al.* 2013). Moreover, TOC decreases with increasing sedimentation rate as an effect of clastic material dilution during fairly stable organic input (Johnson-Ibach 1982; Tromp *et al.* 1995).

Typically for a foreland basin development, a gradual increase in subsidence rate in the BB is observed from the (Middle?) Late Ordovician and continuously throughout the Silurian (particularly in the Ludlow and Pridoli) (Poprawa *et al.* 1999). In this constantly deepening sedimentary basin, prior to the Llandovery-Wenlock boundary the extinction event, Ireviken Event, contributed to oxygen-poor conditions of bottom-water as described by Vanderbroucke *et al.* (2013) and Maier & Servais (2013). In turn, in the Late Silurian the approaching foreland of the Caledonian orogeny became a source of detrital material deposited into the basin from southwest (Poprawa, op. cit.). Therefore, the oxidation rate and organic matter decaying increased (Wilson *et al.* 1986; Buckley & Cranston 1988). Moreover, a global regression in Mid-Homerian (Wenlock, Silurian) times, correlated with climate change may have caused increasing oxidation of bottom-water (Calner, 1999; Jarochowska *et al.* 2016).

In general, to preserve hematite in deep marine sediments, given the results of Liu *et al.* (2004) and Roberts & Weaver (2005), an appearance of more aerobic conditions of bottom-water is necessary. The following factors favour such conditions, and thus the preservation of hematite: higher sedimentation rate, and uplift or sea regression. These conditions were fulfilled during the Caledonian orogeny (Silurian times), where, in the deep sedimentary BB, anoxic conditions associated with the Ireviken extinction event were changed by (1) gradual increasing of sedimentation rate connected with subsidence, related to East-Avalonia collision with Baltica and (2) the sea regression connected with cooling of the climate (Verniers *et al.* 2008).

5.3 Other magnetic minerals

In these rocks we did not detect any signs of pyrrhotite. According to the studies of Aubourg & Pozzi (2010) and Kars *et al.* (2014, 2015) this mineral appears after heating the rocks above 200 °C. This is in line with palaeotemperatures deduced from values of thermal maturity of organic matter of studied mudstones, which do not exceed 1.42 per cent Ro.

6 CONCLUSIONS

Similarly to the Jantar, the Pelplin Formation exhibits the presence of MD or PSD magnetite. In both facies we see the occurrence of MD/PSD magnetite which we interpret as detrital in origin. The suppression of the Verwey transition in mudstones from the Pelplin Formation may be related to the presence of neo-formed SP/SD magnetite grains produced by bacteria, or to the occurrence of detrital titanomagnetite.

The Pelplin Formation (with lower values of TOC) has a different magnetic mineral composition than the Jantar Formation (the 'sweet spot' layer), as the appearance of hematite is documented. Our observations show that hematite appeared at the very early stage of rock formation and/or its diagenesis. We propose that the hematite (mostly SD grains) in mudstones and carbonate concretions, has a detrital origin, likely aeolian, however, an early diagenetic origin is also possible, most probably by chemical processes of volcanic ash in marine water. The preservation of hematite in marine sediments was possible due to the presence of mainly aerobic conditions at the bottom of sedimentary basin, where precipitation of calcareous concretions occurred, and lower concentrations of organic matter are preserved. Moreover, an occurrence of hematite in mudstones and concretions of the Peplin Formation suggests that stable oxic conditions were present at the bottom of the sedimentary basin continuously during deposition of clastic material, cementation and concretions compaction. In turn, the absence of hematite in the Jantar Formation suggests that during sedimentation and early diagenesis more anoxic conditions were present at the bottom.

The absence of pyrrhotite suggests that these rocks were heated to less than 200 °C, which agrees with palaeotemperature known from values of thermal maturity of organic matter (not exceeding 1.42 per cent Ro, which implies a maximal temperature of approximately 150 °C).

As a main conclusion from this paper we suggest that the magnetic mineral assemblages in the studied Silurian shales from Northern Poland are linked with the amount of organic matter. The presence of hematite is related to the significantly lower amount of organic matter in sedimentary rocks, which may be a useful factor in case of the organic matter preservation. However, further investigation to fully recognize this complex problem, should take into consideration (1) rocks containing variable amount of organic matter or (2) different lithology, as well as (3) detailed recognition of minerals origin and (4) exact measurements of organic matter content to compute correlation parameters. We also consider as desirable to conduct an additional measurements, using for instance, geochemical parameters based on elements ratio (e.g. V/(V + Ni), V/Cr), allowing reconstruction of oxygen level, pH and Eh in sediments, to compare with magnetic methods.

ACKNOWLEDGEMENTS

This project was helped by a Visiting Fellowship at the Institute for Rock Magnetism, which is funded by the US National Science Foundation and the University of Minnesota. The visit has been partially financed from the funds of the Leading National Research Centre (KNOW) received by the Centre for Polar Studies for the period 2014–2018. This work has been also funded by the Polish National Centre for Research and Development within the Blue Gas project (No BG2/SHALEMECH/14). Samples were provided by the PGNiG SA. We thank Sara Satolli, Richard Elmore, and Eduard Petrovsky (the Editor), the reviewers whose comments helped improve and clarify this manuscript.

REFERENCES

Algeo, T.J. & Lyons, T.W., 2006. Mo-total organic carbon covariation in modern anoxic marine environments: Implications for analysis of paleoredox and paleohydrographic conditions, *Paleoceanography,* **21**(1), PA1016, doi:10.1029/2004PA001112.

Aragón, R., Buttrey, D.J., Shepherd, J.P. & Honig, J.M., 1985. Influence of nonstoichiometry on the Verwey transition, *Phys. Rev.B.,* **31,** 430–436.

Arnaboldi, M. & Meyers, P.A., 2007. Trace element indicators of increased primary production and decreased water-column ventilation during deposition of latest Pliocene sapropels at five locations across the Mediterranean Sea, *Palaeogeog. Palaeoclimat. Palaeoecol.,* **249**(3-4), 425–443.

Aubourg, C. & Pozzi, J.-P., 2010. Toward a new <250° C pyrrhotite-magnetite geothermometer foe claystones, *Earth Planet. Sci. Lett.,* **294**(1-2), 47–57.

Balsam, W., Damuth, J.E. & Deaton, B., 2007. Marine sediment components: identification and dispersal assessed by diffuse reflectance spectrophotometry, *Int. J. Environment and Health,* Vol. **1,** pp. 403–426, No. 3.

Banerjee, S.K., Hunt, C.P. & Liu, X.-M., 1993, Separation of local signals from the regional paleomonsoon record of the Chinese loess plateau: a rock-magnetic approach, *Geophys. Res. Lett.,* **20,** 843–846.

Blumstein, A.M., Elmore, R.D., Engel, M.H., Elliot, C. & Basu, A., 2004. Paleomagnetic dating of burial diagenesis in Mississippian carbonates, Utah, *J. geophys. Res.,* **109,** 1–16.

Buckley, D.E. & Cranston, R.E., 1988. Early diagenesis in deep sea turbidites: the imprint of paleo-oxidation zones, *Geochim. Cosmochim. Acta.,* **52,** 2925–2939.

Calner, M., 1999. Stratigraphy, facies development, and depositional dynamics of the Late Wenlock Fröjel Formation, Gotland, Sweden, *Geologiska Föreningens i Stockholm Förhandlingar,* **121**(1), 13–24.

Calner, M., 2005. Silurian carbonate platforms and extinction events—ecosystem changes exemplified from Gotland, Sweden, *Facies,* **51**(1-4), 584–591.

Calvert, S.E. & Pedersen, T.F., 1993. Geochemistry of Recent Oxic and Anoxic Marine Sediments: Implications for the Geological Record, *Marine Geology,* **113,** 67–88.

Caricchi, C., Corrado, S., Di Paolo, L., Aldega, L. & Grigo, D., 2015. Thermal maturity of Silurian deposits in the Baltic Syneclise (on-shore Polish Baltic Basin): contribution to unconventional resources assessment, *Ital. J. Geosci.,* **135**(3), 383–393.

Carter-Stiglitz, B.S., Moskowitz, B., Solheid, P., Berquó, T.S., Jackson, M. & Kosterov, A., 2006. Low-temperature magnetic behavior of multidomain titanomagnetites: TM0, TM16, and TM35, *J. geophys. Res. B,* **111**(B12S05), doi:10.1029/2006JB004561.

Chang, L., Heslop, D., Roberts, A.P., Rey, D. & Mohamed, K.J., 2016. Discrimination of biogenic and detrital magnetite through a double Verwey transition temperature, *J. geophys. Res.: Solid Earth,* **121,** 3–14.

Chang, L. *et al.*, 2013. Low-temperature magnetic properties of pelagic carbonates: oxidation of biogenic magnetite and identification of magnetosome chains, *J. geophys. Res.: Solid Earth,* **118**(12), 6049–6065.

Chang, S.-B.R. & Kirschvink, J.L., 1989. Magnetofossils, the magnetization of sediments, and the evolution of magnetite biomineralization, *Ann. Rev. Earth Planet. Sci.,* **17,** 169–195.

Channell, J.E.T., Hodell, D.A., Margari, V., Skinner, L.C., Tzedakis, P.C. & Kesler, M.S., 2013. Biogenic magnetite, detrital hematite, and relative paleointensity in Quaternary sediments from the Southwest Iberian Margin, *Earth planet. Sci. Lett.,* **376,** 99–109.

Day-Stirrat, R., Loucks, R.G., Milliken, K.L., Hillier, S. & van der Pluijm, B., 2008 Phyllosilicate orientation demonstrates early timing of compactional stabilization in calcite-cemented concretions in the Barnett Shale (Late Mississippian), Fort Worth Basin, Texas (U.S.A), *Clays Clay Miner.,* **56,** 100111.

Edwards, C.T., Pufahl, P.K., Hiatt, E.E. & Kyser, K.T., 2012. Paleoenvironmental and taphonomic controls on the occurrence of Paleoproterozoic microbial communities in the 1.88 Ga Ferriman Group, Labrador Trough, Canada, *Precambrian Res.,* **212–213,** 91–106.

Froelich, P.N. *et al.*, 1979. Early oxidation of organic matter in pelagic sediments of the eastern equatorial Atlantic: suboxic diagenesis, *Geochim. Cosmochim. Acta.,* **43,** 1075–1090.

Goldberg, K. & Humayun, M., 2016. Geochemical paleoredox indicators in organic-rich shales of the Irati Formation, Permian of the Paraná Basin, southern Brazil. *Braz. J. Geol.,* **46**(3), 377–393.

Grad, M., Guterch, A. & Mazur, S., 2002. Seismic refraction evidence for crustal structure in the central part of the Trans-European Suture Zone in Poland, Winchester, J. A., Pharaoh, T. C. & Verniers, J.. *Palaeozoic Amalgamation of Central Europe,* Vol. **201,** Geological Society of London, Special Publication, pp. 295–309.

Grotek, I., 1999. The clayey-muddy complex of the Ordovician and Silurian age in the Pomeranian Caledonides belt as well as the Cambrian, *Geological Quarterly,* **43**(3), 297–312 .

Halgedahl, S. & Jarrard, R.D., 1995. Low-temperature behavior of single domain through multidomain magnetite, *Earth planet. Sci. Lett.,* **130,** 127–139.

Hatfield, R.G., 2014. Particle size-specific magnetic measurements as a tool for enhancing our understanding of the bulk magnetic properties of sediments, *Minerals,* **4,** 758–787

Hrouda, F., 1994. A technique for the measurement of thermal changes of magnetic susceptibility of weakly magnetic rocks by the CS-2 apparatus and KLY-2 Kappabridge, *Geophys. J. Int.,* **118**(3), 604–612.

Hrouda, F., Jelinek, V. & Zapletal, K., 1997. Refined technique for susceptibility resolution into ferromagnetic and paramagnetic components bases on susceptibility temperature variations measurement, *Geophys. J. Int.,* **129**(3), 715–719.

Jackson, M., Bowles, J. & Banerjee, S., 2011. Interpretation of low temperature data. Part V: the magnetite verwey transition (Part B): field-cooling effects on stoichiometric magnetite below TV, *IRM Quart.,* **21**(4), 1–11.

Jackson, M. & Solheid, P., 2010. On the quantitative analysis and evaluation of magnetic hysteresis data, *Geochem. Geophys. Geosyst.,* **11,** Q04Z15, doi:10.1029/2009GC002932.

Jarochowska, E., Munnecke, A., Frisch, K., Ray, D.C. & Castagner, A., 2016. Faunal and facies changes through the mid Homerian (late Wenlock, Silurian) positive carbon isotope excursion in Podolia, western Ukraine, *Lethaia,* **49,** 170–198.

Jaworowski, K., 2002. Profil dolnego paleozoiku w północnej Polsce - zapis kaledońskiego stadium rozwoju basenu bałtyckiego. *Pos. Nauk. Państw. Inst. Geol.,* **58,** 9–10.

Johnson-Ibach, L.E., 1982. Relationship between sedimentation rate and total-organic carbon content in ancient marine sediments, *Am. Assoc. Petrol. Geol. Bull.,* **66,** 170–188.

Karcz, P., Janas, M. & Dyrka, I., 2013. Polish shale gas deposits in relation to selected shale gas prospective areas of Central and Eastern Europe, *Przegląd Geologiczny,* **61,** 608–620.

Karlin, R. & Levi, S., 1983. Diagenesis of magnetic minerals in Recent haemipelagic sediments, *Nature,* **303,** 327–330.

Karlin, R. & Levi, S., 1985. Geochemical and sedimentological control of the magnetic properties of hemipelagic sediments, *J. geophys. Res.,* **90**(B12), 10 373–10 392.

Kars, M., Aubourg, C., Labaume, P., Bierquó, T. & Cavailhes, T., 2014. Burial diagenesis of magnetic minerals: new insights from the Grès d'Annot Transect (SE France), *Minerals,* **4,** 667–689.

Kars, M., Aubourg, C., Labaume, P., Bierquó, T. & Cavailhes, T., 2014. Burial diagenesis of magnetic minerals: New insights from the Grès d'Annot Transect (SE France), *Minerals,* **4**(3), 667–689.

Kars, M., Aubourg, C. & Suárez-Ruiz, I., 2015. Neoformed magnetic minerals as an indicator of moderate burial: the key example of middle Paleozoic sedimentary rocks, West Virginia, *AAPG Bull.,* **99**(3), 389–401.

Kars, M., Aubourg, C. & Suárez-Ruiz, I., 2015. Neoformed magnetic minerals as an indicator of moderate burial: The key example of middle Paleozoic sedimentary rocks, West Virginia, *AAPG Bulletin,* **99**(03), 389–401.

Katz, B., Elmore, R.D., Cogoini, M., Engel, M.H. & Ferry, S., 2000. Associations between burial diagenesis of smectite, chemical remagnetization, and magnetite authigenesis in the Vocontian trough, SE France, *J. geophys. Res.,* **105**(B1), 851–868.

Kiipli, E., 2004. Redox changes in the deep shelf of the East Baltic Basin in the Aeronian and early Telychian (early Silurian), *Proc. Estonian Acad. Sci. Geol.,* **53**(2), 94–124.

Kiipli, E., Kallaste, T. & Kiipli, T., 2000. Hematite and goethite in Telychian marine red beds of the East Baltic, *GFF,* **122**(3), 281–286.

Kirschvink, J.L. & Chang, S.-B.R., 1984. Ultrafine-grained magnetite in deep-sea sediments: possible bacterial magnetofossils, *Geology,* **12**(9), 559–562.

Kletetschka, G. & Wasilewski, P.J., 2002. Grain size limit for SD hematite, *Phys. Earth planet. Inter.,* **129,** 173–179.

Kowalski, A., Więcław, D., Grotek, I., Kotarba, M.J. & Kosakowski, P., 2010. Habitat and hydrocarbon potential of the lower Paleozoic source rocks in the Polish part of the Baltic region, *Geol. Quart.,* **54**(2), 159–182.

Kruiver, P.P., Dekkers, M.J. & Heslop, D., 2001. Quantification of magnetic coercivity components by the analysis of acquisition curves of isothermal

remanent magnetisation, *Earth and Planetary Science Letters,* **189**(3-4), 269–276.

Kąkol, Z. & Honig, J.M., 1989. Influence of deviations from ideal stoichiometry on the anisotropy parameters of magnetite Fe3(1-*δ*)O4, *Physical Review B,* **40,** 9090–9097.

Kąkol, Z., Sabol, J., Stickler, J., Kozłowski, A. & Honig, J.M., 1992. Influence of titanium doping on the magnetocrystalline anisotropy of magnetite, *Phys. Rev. B,* **49,** 12 767–12 772.

Labuhn, I. *et al.*, 2018. Holocene Hydroclimate Variability in Central Scandinavia Inferred from Flood Layers in Contourite Drift Deposits in Lake Storsjön, *Quaternary,* **1**(1), 2.

Lash, G.G., 2015. Authigenic barite nodules and carbonate concretions in the Upper Devonian shale succession of western New York—A record of variable methane flux during burial, *Marine and Petroleum Geology,* **59,** 305–319.

Lash, G.G. & Blood, D.R., 2004. Geochemical and textural evidence for early (shallow) diagenetic growth of stratigraphically confined carbonate concretions, Upper Devonian Rhinestreet black shale, western New York, *Chemical Geology,* **206**(3-4), 407–424.

Lazauskiene, J., Sliaupa, S., Brazauskas, A. & Musteikis, P., 2003. Sequence stratigraphy of the Baltic Silurian succession: tectonic control on the foreland infill, *Geol. Soc., Lond. Spec. Publ.,* **208,** 95–115.

Liu, J., Zhu, R., Roberts, A., Li, S. & Chang, J., 2004. High-resolution analysis of early diagenetic effects on magnetic minerals in post-middle-Holocenecontinental shelf sediments from the Korea Strait, *J. Geophys. Res.,* **109,** B03103.

Liu, Q.S., Jackson, M., Banerjee, S.K., Zhu, R.X., Pan, Y.X. & Chen, F.H., 2003. Determination of magnetic carriers of the characteristic remanent magnetization of Chinese loess by low-temperature demagnetization, *Earth planet. Sci. Lett.,* **216**(1-2), 175–186.

Lovley, D.R., Stoltz, J.F., Nord, G.L. & Phillips, E.J.P., 1987. Anaerobic production of magnetite by a dissimilatory iron-reducing microorganism, *Nature,* **330,** 252–254.

Maier, G. & Servais, T., 2013. Reconstructing the environmental conditions around the Silurian Ireviken Event using the carbon isotope composition of bulk and palynomorph organic matter, *Geochem. Geophys. Geosyst.,* **14,** 86–101.

Manning, E.B. & Elmore, R.D., 2015. An integrated paleomagnetic, rock magnetic, and geochemical study of the Marcellus shale in the Valley and Ridge province in Pennsylvania and West Virginia, *J. geophys. Res.: Solid Earth,* **120,** 705–724.

Mastalerz, M., Schimmelmann, A., Drobniak, A. & Chen, Y., 2013. Porosity of Devonian and Mississippian New Albany Shale across a maturation gradient: insights from organic petrology', gas adsorption, and mercury intrusion, *Am. Assoc. Petrol. Geol. Bull.,* **97,** 1621–1643.

Meyers, P.A. & Shaw, T.J., 1996. Organic matter accumulation, sulfate reduction, and methanogenesis in pliocene-pleistocene turbidites on the Iberia Abyssal Plain, in *Proceedings of the Ocean Drilling Program,* Vol. **149,** pp. 705–712, eds Whitmarsh, R.B., Sawyer, D.S., Klaus, A. & Masson, D.G., Scientific Results.

Meyers, S.R., Sageman, B.B. & Lyons, T.W., 2005. Organic carbon burial rate and the Molybdenum proxy: Theoretical framework and application to Cenomanian-Turonian Oceanic Anoxic Event 2, *Paleoceanography,* **20**(2), PA2002, doi:10.1029/2004PA001068.

Modliński, Z., 1976. Niektóre zagadnienia strukturalne zachodniej części syneklizy perybałtyckiej, *Biuletyn Instytutu Geologicznego,* **270,** Z badań geologicznych Niżu Polskiego, II, 37–44.

Modliński, Z. & Podhalańska, T., 2010. Outline of the lithology and depositional features of the Lower Paleozoic strata in the Polish part of the Baltic region, *Geol. Quart.,* **54,** 109–121.

Modliński, Z., Szymański, B. & Teller, L., 2006. Litostratygrafia syluru polskiej części obniżenia perybałtyckiego - część lądowa i morska (N Polska), *Przegląd Geol.,* **54,** 787–796.

Morad, S. & Aldahan, A.A., 1986. Alteration of detrital Fe-Ti oxides in sedimentary rocks, *Bull. geol. Soc. Am.,* **97**(5), 567–578.

Moskowitz, B.M., Frankel, R.B. & Bazylinski, D.A., 1993. Rock magnetic criteria for the detection of biogenic magnetite, *Earth planet. Sci. Lett.,* **120,** 283–300.

Moskowitz, B.M., Jackson, M. & Kissel, C., 1998. Low-temperature magnetic behavior of titanomagnetites, *Earth planet. Sci. Lett.,* **157,** 141–149.

Murray, J.W., 1979. Iron oxides,in *Marine Minerals,* pp. 47–98, ed. Burns, R.G. Am. Mineral. Soc.

Niezabitowska, D.K., Szaniawski, R., Roszkowska-Remin, J. & Gąsiński, A., 2019, Magnetic Anisotropy in Silurian Gas-Bearing Shale Rocks from the Pomerania Region (Northern Poland), *J. geophys. Res.: Solid Earth,* **124**(1), 5–25.

Nord, G.L., Jr. & Lawson, C.A., 1989. Order-disorder transition-induced twin domains and magnetic properties in ilmenite-hematite, *Am. Mineral.,* **74,** 160–176.

Oliva-Urcia, B., Pueyo, E.L. & Larrasoana, J.C., 2008. Magnetic reorientation induced by pressure solution: a potential mechanism for orogenic-scale remagnetizations. *Earth planet. Sci. Lett.,* **265,** 525–534.

Passier, H.F. & Dekkers, M.J., 2002. Iron oxide formation in the active oxidation front above sapropel S1 in the eastern Mediterranean Sea as derived from low-temperature magnetism, *Geophys. J. Int.,* **150,** 230–240.

Petersen, N., von Dobeneck, T. & Vali, H., 1986. Fossil bacterial magnetite in deep-sea sediments from the South Atlantic Ocean, *Nature,* **3**(20), 611–615.

Poprawa, P., 2010. Potencjał występowania złóż gazu ziemnego w łupkach dolnego paleozoiku w basenie bałtyckim i lubelsko-podlaskim, *Przegląd Geol.,* **58**(3), 226–249.

Poprawa, P., Šliaupa, S., Stephenson, R.A. & Lazauskienë, J., 1999. Late Vendian-Early Palaeozoic tectonic evolution of the Baltic Basin: regional implications from subsidence analysis, *Tectonophysics,* **314,** 219–239.

Raiswell, R., Buckley, F., Berner, R.A. & Anderson, T.F., 1988. Degree of pyritization of iron as a paleoenvironmental indicator of bottom-water oxygenation, *J. Sediment. Res.,* **58**(5), 812–819.

Rhoads, D.C. & Morse, J.W., 1971. Evolutionary and ecologic significance of oxygen-deficient marine basins, *Lethaia,* **4**(4), 413–428.

Roberts, A.P. & Pillans, B.J., 1993. Rock magnetism of Lower/Middle Pleistocene marine sediments, Wanganui Basin, New Zealand, *Geophys. Res. Lett.,* **20,** 839–842.

Roberts, A.P. & Turner, G.M., 1993. Diagenetic formation of ferrimagnetic iron sulphide minerals in rapidly deposited marine sediments, South Island, New Zealand, *Earth planet. Sci. Lett.,* **115**(1–4), 257–273.

Roberts, A.P. & Weaver, R., 2005. Multiple mechanisms of remagnetization involving sedimentary greigite (Fe3S4), *Earth planet. Sci. Lett.,* **231,** 263–277.

Sageman, B.B., Murphy, A.E., Werne, J.P., Straeten, C.A.V., Hollander, D.J. & Lyons, T.W., 2003. A tale of shales: the relative roles of production, decomposition, and dilution in the accumulation of organic-rich strata, Middle-Upper Devonian, Appalachian Basin, *Chem. Geol.,* **195**(1-4), 229–273.

Schulz, H.D., Dahmke, A., Schinzel, U., Wallmann, K. & Zabel, M., 1994. Early diagenetic processes, fluxes, and reaction rates in sediments of the South Atlantic, *Geochim. Cosmochim. Acta,* **58,** 2041–2060.

Scotese, C., 2001. *Atlas of Earth History, Vol. 1, Paleogeography,* PALEOMAP Project, pp. 58, ISBN: 0-9700020-0-9.

Smirnov, A.V. & Tarduno, J.A., 2001. Estimating superparamagnetism in marine sediments with the time-dependency of coercivity of remanence, *J. geophys. Res.,* **106,** 16135–16144.

Syono, Y., 1965. Magnetocrystalline anisotropy and magnetostriction of Fe3O4-Fe2TiO4 series, with special application to rock magnetism, *Jpn. J. Geophys.,* **4,** 71–143.

S´rodon´, J. & Clauer, N., 2001. Diagenetic history of Lower Palaeozoic sediments in Pomerania (northern Poland), traced across the Teisseyre–Tornquist tectonic zone using mixed-layer illite-smectite, *Clay Miner.,* **36**(1), 15–27.

Tarduno, J.A., 1995. Superparamagnetism and reduction diagenensis in pelagic sediments: Enhancement or depletion?, *Geophys. Res. Lett.,* **22,** 1337–1340.

Tari, G., Poprawa, P. & Krzywiec, P., 2012. *Silurian Lithofacies and Paleogeography in Central and Eastern Europe: Implications for Shale Gas Exploration,* Society of Petroleum Engineers – SPE 151606.

Torsvik, T.H., Robin, L. & Cocks, M., 2017. *Earth History and Palaeogeography,* Cambridge University Press, doi:10.1017/9781316225523.

Trabucho-Alexandre, J., Dirkx, R., Veld, H., Klaver, G. & de Boer, P.L., 2012. Toarcian black shales in the Dutch Central Graben: record of energetic, variable depositional conditions during an oceanic anoxic event, *J. Sediment. Res.,* **82**(2), 104–120.

Tromp, T.K., Van Cappellen, P. & Key, R.M., 1995. A global model for the early diagenesis of organic carbon and organic phosphorus in marine sediments, *Geochim. Cosmochim. Acta.,* **59,** 1259–1284.

Uhlein, A., Alvarenga, C.J.S., Dardenne, M.A. & Trompette, R.R., 2011. The glaciogenic Jequitai Formation, southeastern Brazil, in *The Geological Record of Neoproterozoic Glaciations,* eds Arnaud, E., Halverson, G.P. & Shields-Zhou, G., Geological Society of London.

Vanderbroucke, T.R.A., Munnecke, A., Leng, M.J., Bickert, T., Hints, O., Gelsthorpe, D., Maier, G. & Servais, T., 2013. Reconstructing the environmental conditions around the Silurian Ireviken Event using the carbon isotope composition of bulk and palynomorph organic matter. *Geochem. Geophys. Geosyst.,* **14,** 86–101.

Verniers, J., Maletz, J., Kříž, J., Žigait, Ž., Paris, F., Schönlaub, H.P. & Wrona, R., 2008. Silurian. in *Geology of the Central Europe,* **Vol. 1: Precambrian and Palaeozoic,** pp. 249–302, ed.McCann. The Geological Society London.

Wilson, T.R.S., Thomson, J., Hydes, D.J., Colley, S., Culkin, F. & Sorensen, J., 1986. Oxidation fronts in pelagic sediments: diagenetic formation of metal-rich layers, *Science,* **232,** 972–975.

Wood, R.A., Lewis, M.H., Lees, M.R., Bennington, S.M., Cain, M.G. & Kitamura, N., 2002. Ferromagnetic fullerene, *J. Phys. Condens. Matter,* **14,** 22.

Zdanavičiūtė, O. & Lazauskienė, J., 2009. Organic matter of Early Silurian succession – the potential source of unconventional gas in the Baltic Basin (Lithuania), *Baltica,* **22**(2), 89–98.

Zegers, T.E., Dekkers, M.J. & Bailly, S., 2003. Late Carboniferous to Permian remagnetization of Devonian limestones in the Ardennes: role of temperature, fluids, and deformation. *J. geophys. Res.,* **108,** doi:10.1029/2002JB002213.

Özdemir, Ö. & Dunlop, D.J., 2010. Hallmarks of maghemitization in low-temperature remanence cycling of partially oxidized magnetite nanoparticles, *J. geophys. Res. B,* **115**(B02101), doi:10.1029/2009JB006756.

Özdemir, Ö., Dunlop, D.J. & Berquó, T.S., 2008. Morin transition in hematite: Size dependence and thermal Hysteresis, *Geochem. Geophys. Geosyst.,* **9**(10), Q10Z01, doi:10.1029/2008GC002110.

Özdemir, Ö., Dunlop, D.J. & Moskowitz, B.M., 1993. The effect of oxidation on the Verwey transition in magnetite, *Geophys. Res. Lett.,* **20,** 1671–1674.